

Electron capture and transport mediated by lattice solitons

D. Hennig,^{1,2} A. Chetverikov,¹ M. G. Velarde,¹ and W. Ebeling^{1,2}

¹*Instituto Pluridisciplinar, Universidad Complutense, Paseo Juan XXIII, 1, 28040 Madrid, Spain*

²*Institut für Physik, Humboldt-Universität Berlin, Newtonstrasse 15, 12489 Berlin, Germany*

(Received 14 May 2007; published 3 October 2007)

We study electron transport in a one-dimensional molecular lattice chain. The molecules are linked by Morse interaction potentials. The electronic degree of freedom, expressed in terms of a tight binding system, is coupled to the longitudinal displacements of the molecules from their equilibrium positions along the axis of the lattice. More specifically, the distance between two sites influences in an exponential fashion the corresponding electronic transfer matrix element. We demonstrate that when an electron is injected in the undistorted lattice it causes a local deformation such that a compression results leading to a lowering of the electron's energy below the lower edge of the band of linear states. This corresponds to self-localization of the electron due to a polaronlike effect. Then, if a traveling soliton lattice deformation is launched a distance apart from the electron's position, upon encountering the polaronlike state it captures the latter dragging it afterwards along its path. Strikingly, even when the electron is initially uniformly distributed over the lattice sites a traveling soliton lattice deformation gathers the electronic amplitudes during its traversing of the lattice. Eventually, the electron state is strongly localized and moves coherently in unison with the soliton lattice deformation. This shows that for the achievement of coherent electron transport we need not start with the polaronic effect.

DOI: [10.1103/PhysRevE.76.046602](https://doi.org/10.1103/PhysRevE.76.046602)

PACS number(s): 63.20.Ry, 63.20.Kr

I. INTRODUCTION

In their pioneering studies of charge transport in molecular systems Landau [1] and Pekar [2] introduced the concept of self-trapped states. This involves an electron accompanied by the lattice deformation. It creates thus a localized quasi-particle compound also called a polaron. Davydov showed that, when the size of the polaron is large enough that the continuum approximation can be applied to the underlying lattice system, a mobile self-trapped state can travel as a solitary wave along the molecular structure [3]. The electron was assumed to be under tight binding by the lattice, hence a nonlinear coupling. Since the work of Davydov in the 1970s the relevance of solitons and/or polarons to the energy and particle transport in macromolecules has been recognized and has remained of great interest (see, e.g., Refs. [4,5]). Most of the studies of transport properties in macromolecules have been based on one-dimensional lattice models. Later Davydov generalized the idea of solitonic exciton transport always considering harmonic hence infinitesimal lattice vibrations to include also charge transport in proteins leading to the term “electro-soliton” [6]. The soliton's stability is the result of the attained balance between two competing mechanisms, namely the interaction between an excitonic degree of freedom and the lattice vibrations of a molecular chain and, on the other hand, the lattice dispersion. The theory of the solitonlike electron transport mechanism in one-dimensional chain models of biomolecules is described in Refs. [5,6]. If anharmonicity is included to account for finite amplitude lattice vibrations in the description of the lattice vibrations either by adding higher-order terms to the potential or considering potentials with strong repulsive parts, represented, e.g., by Toda and Morse potentials [7,8] the lattice dynamics itself can support supersonic solitons. The latter can accommodate matter or charge transport

[9] and excitonic energy or self-trapping modes establishing transfer beyond the subsonic regime [10–22]. Such electron trapping by the soliton leads to a dynamic bound state that was called “solelectron” in Ref. [11]. Note that the nonlinearity of the “electro-soliton” comes from the above-mentioned electron-lattice tight binding interaction while for the “solelectron” the nonlinearity originates in the lattice dynamics alone, with or without charges. The interacting pair “electro-soliton”-soliton is what the “solelectron” becomes when the classical charge is replaced by a quantum electron with tight binding description. Accordingly there are two types of nonlinearity and hence two different transport mechanisms not necessarily providing the same effect, as already noted in Refs. [10,17]. It should be mentioned that due to the fairly strong electronic coupling the electron transport considered in this paper can indeed be adiabatic. In the limit of weak electronic coupling the nonadiabatic regime of electron transfer is relevant as described by the Marcus theory [18,19].

The aim of the present work is to elaborate on the capture mechanism of solitonic lattice deformations. In particular we aim to clarify whether coherent electron transport is achievable although a lattice soliton is launched a distance away from the injected electron. A further aspect is possible restoring of localization for an initially completely distributed electron through passing lattice solitons. In Sec. II we pose the problem by introducing the Hamiltonian for the electron and the lattice dynamics and define the electron-lattice coupling thus leading to the equations of motion. The latter are integrated for various initial conditions and the results are provided in Sec. III. Finally, in Sec. IV we summarize the major results found.

II. DYNAMICAL SYSTEM

We investigate a one-dimensional lattice chain of molecules coupled by Morse forces [8] in which one excess elec-

tron has been injected. Our model Hamiltonian of charge transport in the system consists of the following two parts:

$$H = H_{el} + H_{lattice}. \quad (1)$$

H_{el} describes quantum mechanically the electron transport over the molecules in the context of a tight-binding system and $H_{lattice}$ represents the classical dynamics of longitudinal vibrations of the molecules, viz. the deformations of the corresponding bonds between them. The electronic tight-binding system is given by

$$H_{el} = - \sum_n V_{nn-1} (c_n^* c_{n-1} + c_n c_{n-1}^*). \quad (2)$$

The index n denotes the site of the n th molecule on the chain and $|c_n|^2$ determines the probability to find the electron (charge) residing at this site. V_{nn-1} is the transfer matrix element (its value is determined by an overlap integral) being responsible for the nearest-neighbor transport of the electron along the chain.

The lattice part of the Hamiltonian, $H_{lattice}$, models dynamical longitudinal changes of the equilibrium positions of the molecules yielding alterations of the length of bonds. The dynamics can appropriately be modeled by Morse potentials [10,12,15,24]. The Hamiltonian of the $H_{lattice}$ is given by

$$H_{lattice} = \sum_n \left\{ \frac{p_n^2}{2M} + D \{ 1 - \exp[-B(q_n - q_{n-1})] \}^2 \right\}. \quad (3)$$

The coordinates q_n quantify the displacements of the molecules from their equilibrium positions along the molecular axis. D is the breakup energy of a bond, B is the range parameter of the Morse potential (the stiffness), and M denotes the mass of a molecular unit. The Morse potential exhibits an exponential-repulsive part preventing the crossover of neighboring lattice particles (molecules) for large displacements. Note that, with an expansion of the exponential functions, one recovers in lowest order the harmonic limit and taking into account higher-order terms anharmonic potentials, as currently done in condensed matter physics [25–27].

The interaction between the electronic and the vibrational degrees of freedom yields modifications of the electronic parameters V_{nn-1} due to the displacements of the molecules from their equilibrium positions. To be precise, the transfer matrix elements V_{nn-1} are supposed to depend on the relative distance between two consecutive molecules on the chain in the following exponential fashion:

$$V_{nn-1} = V_0 \exp[-\alpha(q_n - q_{n-1})]. \quad (4)$$

The quantity α regulates how strong V_{nn-1} is influenced by the distance, $r_n = q_n - q_{n-1}$, or in other words it determines the coupling strength between the electron and the lattice system. On the other hand the actual charge occupation has its (local) impact on the longitudinal distortion of the molecular chain (the polaronlike effect). Note that here the exponential form of the electron-lattice interaction accounts for both small and large displacements of the lattice units thus going beyond the range of harmonic interaction considered in earlier studies [3,5,15–17,24–33].

For universality in the arguments we pass to a dimensionless representation by introducing suitable scales. Time is scaled as $\tilde{t} = \Omega_{Morse} t$, with $\Omega_{Morse} = \sqrt{2D B^2 / M}$ being the frequency of harmonic oscillations around the minimum of the Morse potential. The energy of the system is measured in units of the depth of the Morse potential, i.e., $H \rightarrow H / (2D)$. The dimensionless representation of the remaining variables and parameters of the system follows from the relations:

$$\tilde{q}_n = B q_n, \quad \tilde{p}_n = \frac{p_n}{\sqrt{2MD}}, \quad \tilde{V} = \frac{V_0}{2D}, \quad (5)$$

$$\tilde{\alpha} = \frac{\alpha}{B}. \quad (6)$$

In what follows we drop the tildes.

The equations of motion derived from the Hamiltonian given in Eqs. (2) and (3) read as

$$i \frac{dc_n}{dt} = -\tau \{ \exp[-\alpha(q_{n+1} - q_n)] c_{n+1} + \exp[-\alpha(q_n - q_{n-1})] c_{n-1} \}, \quad (7)$$

$$\begin{aligned} \frac{d^2 q_n}{dt^2} = & [1 - \exp\{- (q_{n+1} - q_n)\}] \exp[- (q_{n+1} - q_n)] \\ & - [1 - \exp\{- (q_n - q_{n-1})\}] \exp[- (q_n - q_{n-1})] \\ & - \alpha V \{ (c_{n+1}^* c_n + c_{n+1} c_n^*) \exp[-\alpha(q_{n+1} - q_n)] \\ & - (c_n^* c_{n-1} + c_n c_{n-1}^*) \exp[-\alpha(q_n - q_{n-1})] \}. \end{aligned} \quad (8)$$

The adiabaticity parameter $\tau = V / (\hbar \Omega_{Morse})$, appearing in the right-hand side of Eq. (7) determines the degree of time scale separation between the (fast) electronic and (slow) acoustic phonon processes. For illustration we use (unless stated otherwise) the following values: $\tau = 10$, $V = 0.1$, and $\alpha = 1.75$ which are relevant for electron transport in hydrogen bonded chains of biomolecules [5,6,22].

Being interested in the simulation of a nonlinear charge transport mechanism we construct as a first step localized stationary solutions of the coupled system [Eqs. (7) and (8)] where we use an adiabatic approach [22]. To this end we note that due to the fact that the lattice motion is slow compared to the electron motion (large adiabaticity parameter τ) the inertia in Eq. (8) are negligible. Moreover, solutions of the stationary Schrödinger equation, associated with a standing electron, are obtained from Eq. (7) with the substitution $c_n(t) = \phi_n \exp(-i\omega t)$ with real-valued amplitudes ϕ_n and where ω is the corresponding spectral parameter. The energy of the system is then given by

$$E = \sum_n \left\{ \frac{1}{2} \{ 1 - \exp[-(q_n - q_{n-1})] \}^2 - V \exp[-\alpha(q_n - q_{n-1})] (\phi_n^* \phi_{n-1} + \phi_n \phi_{n-1}^*) \right\}, \quad (9)$$

and the stationary equations are derived according to

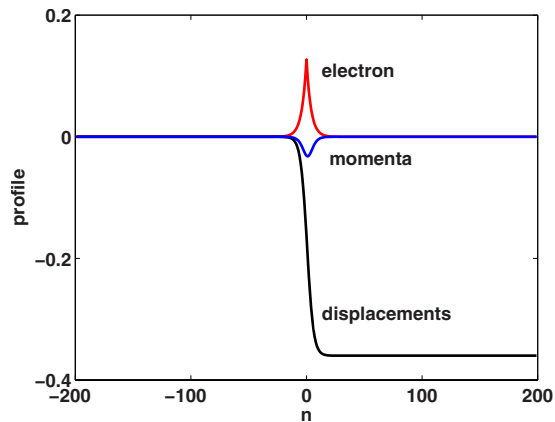


FIG. 1. (Color online) Initial profile of the localized electron state and lattice deformation realizing a minimum of the variational energy. Also shown is the pattern of the momenta used to activate lattice soliton motion. The parameter values are $V=0.1$ and $\alpha=1.75$.

$$\frac{\partial E}{\partial q_n} = 0, \quad \frac{\partial}{\partial \phi_n} \left(E + \omega \sum_n \phi_n^2 \right) = 0. \quad (10)$$

Solutions of the Morse chain are supposed to be of the form of the Toda-soliton

$$\exp[-(q_n - q_{n-1})] = 1 + \sinh^2 \kappa \cosh^{-2}(\kappa n), \quad (11)$$

where κ is treated as a variational parameter. For the localized electronic solution we use a simple trial function

$$\phi_n = A \eta^{|n|}, \quad (12)$$

where the variational parameter $0 < \eta < 1$ gives the width of the solution. The closer η is to the value $\eta \rightarrow 1$ the more delocalized the state becomes. Correspondingly, for $\eta \rightarrow 0$ the state gets more localized. The coefficient A follows from the normalization condition and is evaluated as

$$A = \sqrt{\frac{1 - \eta^2}{1 + \eta^2}}. \quad (13)$$

The total variational energy is then expressed as

$$\Gamma = \frac{1}{2} \sum_n \frac{\sinh^4 \kappa}{\cosh^4(\kappa n)} - 2V \frac{1 - \eta^2}{1 + \eta^2} \sum_n \left(1 + \frac{\sinh^2 \kappa}{\cosh^2(\kappa n)} \right)^\alpha \eta^{|n|} \eta^{|n-1|}. \quad (14)$$

For a given set of system parameters α and V the global minimum of Γ , giving the lowest energy configuration, is searched for in the two-parameter space (κ, η) . A typical initial electronic state and profile of displacements of the molecules are depicted in Fig. 1. The corresponding localized compound is comprised of an exponentially localized electron state and the associated kink-shape topological lattice deformation. The latter is in the forthcoming referred to as the lattice soliton. Motion of the lattice soliton is achieved with the excitation of the momenta according to the gradient

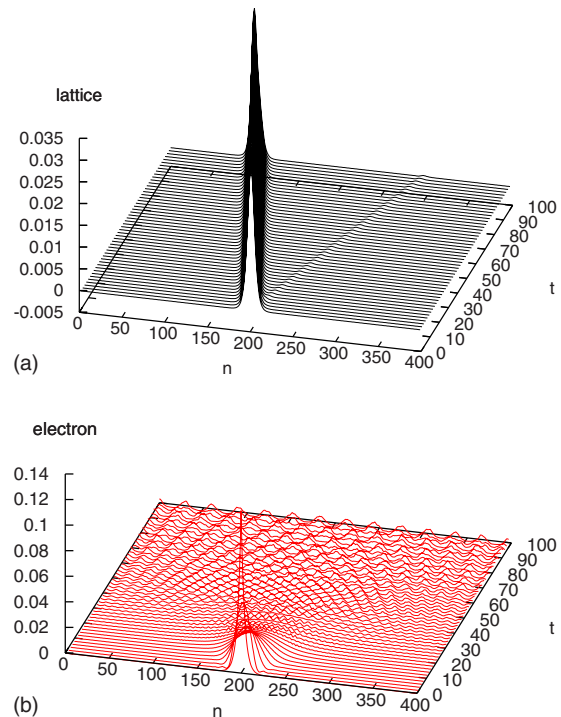


FIG. 2. (Color online) Spatiotemporal pattern of a lattice soliton (top panel) and an initially localized electron state (bottom panel). The parameter values are $V=0.1$ and $\alpha=0$.

method [23] yielding the soliton momentum profile shown in Fig. 1.

III. NUMERICAL RESULTS

Before we embark on a study of the coupled electron lattice dynamics it is illustrative to consider first the limiting case of zero coupling ($\alpha=0$) for which the initially localized electron state and a lattice soliton evolve independently as displayed in Fig. 2. To activate soliton motion an initial pattern of the momenta of appropriate shape is imposed (cf. Fig. 1). We integrated the system [Eqs. (7) and (8)] using a fourth-order Runge-Kutta scheme where we imposed periodic boundary conditions. Accuracy of our computations was guaranteed by monitoring the conservation of the norm $\sum_n |c_n(t)|^2 = 1$ as well as the conservation of the total energy. Obviously, the electron's occupation probability, being peaked initially at the central lattice site, decays in the course of time. Eventually, the electron, whose temporal evolution is described by a tight-binding equation alone, is spread all over the lattice. In clear contrast is the behavior of the lattice soliton, represented as $\exp[-(q_n - q_{n-1})]$, which moves, apart from the emission of a tiny amplitude linear wave (phononic radiation), form-invariant and with constant velocity over the lattice chain. This shows that the pure lattice deformation can be coherently moved along the lattice in a solitonlike fashion by appropriately exciting the momenta.

Further illustration of the spatial spreading of the electronic wave function is given in Fig. 3 where the temporal behavior of the electronic partition number is drawn. The latter is defined as

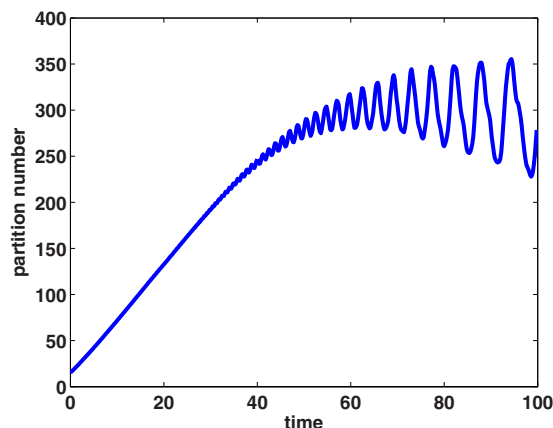


FIG. 3. (Color online) Time evolution of the electronic partition number with initial conditions and parameter values as in Fig. 2.

$$P(t) = \sum_{n=1}^N \frac{|c_n(0)|^4}{|c_n(t)|^4}. \tag{15}$$

Due to the normalization of $\sum_{n=1}^N |c_n|^2 = 1$ complete localization at a single site is given for $P=1$ whereas the electron is uniformly extended over the lattice for $P=N$, that is, P measures the number of lattice sites that are occupied by the electron. For times up to $t \sim 40$ there is a linear growth of $P(t)$ and afterwards oscillations with rising amplitudes result. Clearly, at the end of our simulation time the electron is almost completely delocalized.

Now we consider interactions between the electron and the lattice system. Let us first display the electron transport mediated by lattice solitons for the situation when the localized electron state and the lattice soliton are centered at the same lattice site [21,22]. The electron and the lattice soliton, after having emitted linear waves of small amplitude (the above-mentioned radiation), travel together with constant velocity along the lattice maintaining both their localized shape (cf. Fig. 4). Note the reduction of the velocity of the bound state compared with the velocity of sound $s_0=1$ in the bare lattice. In this manner stable soliton mediated coherent electron transport is realized. That the electron and lattice soliton move in unison is also seen in Fig. 5 showing the first momentum of the electronic occupation probability and the center of the lattice soliton. Thus we can infer (see also Ref. [22]) that the coupling interaction between the electron and the lattice soliton is not only crucial for the preservation of the electron localization but it is also responsible for the dragging of the electron by the lattice soliton.

We stress the *local character of the electron-lattice interaction* in the previous case, viz. initially the peak of the electronic occupation probability and the center of the lattice soliton coincide so that most efficient electron-lattice coupling from the start is guaranteed. However, one can imagine situations for which the injected excess electron is a distance apart from the region where a solitonic lattice deformation has been launched (e.g., by an imposed local pressure, a defect, or a thermally induced hot spot). We consider now such cases when the centers of the localized electron state

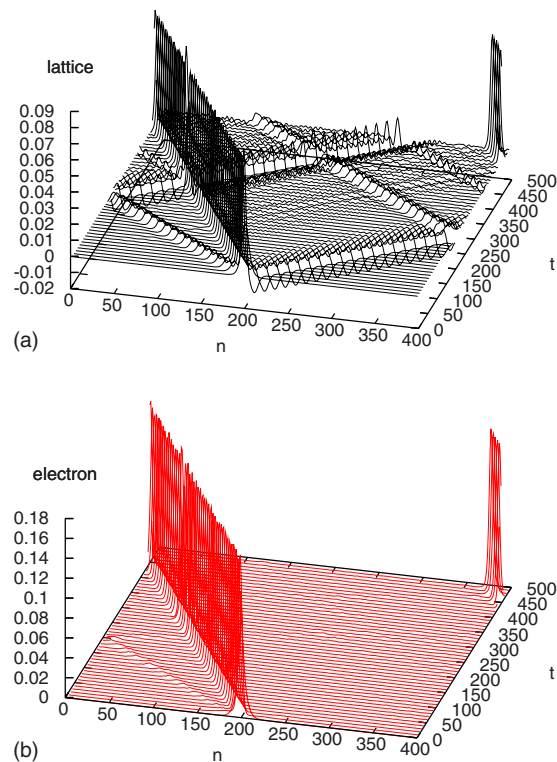


FIG. 4. (Color online) Spatiotemporal pattern of a lattice soliton (top panel) coupled with a localized electron state (bottom panel). Both excitations are launched at the center of the lattice. The parameter values are $V=0.1$ and $\alpha=1.75$.

and the lattice soliton do not coincide initially. The question is then: Is coherent electron transport achievable at all under such a seemingly disadvantageous circumstance, especially when the degree of interaction between the electron and the soliton lattice deformation seems to be lessened due to the rather large initial distance between their excitation peaks. In Fig. 6 we illustrate the spatiotemporal patterns of the occupation probability of the electron and the amplitude of the lattice soliton, respectively. In the beginning the electron and

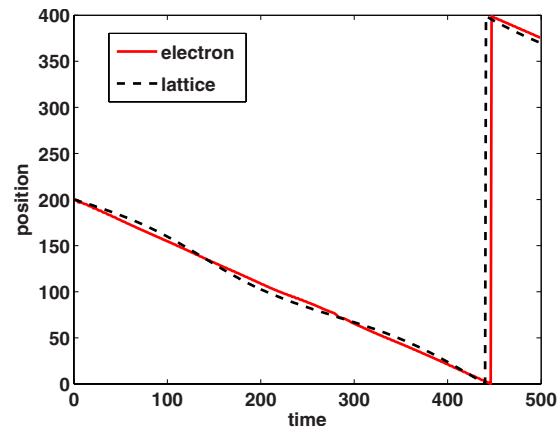


FIG. 5. (Color online) Time evolution of the first momentum of the electronic occupation probability and the center of the lattice soliton. Parameter values as in Fig. 4.

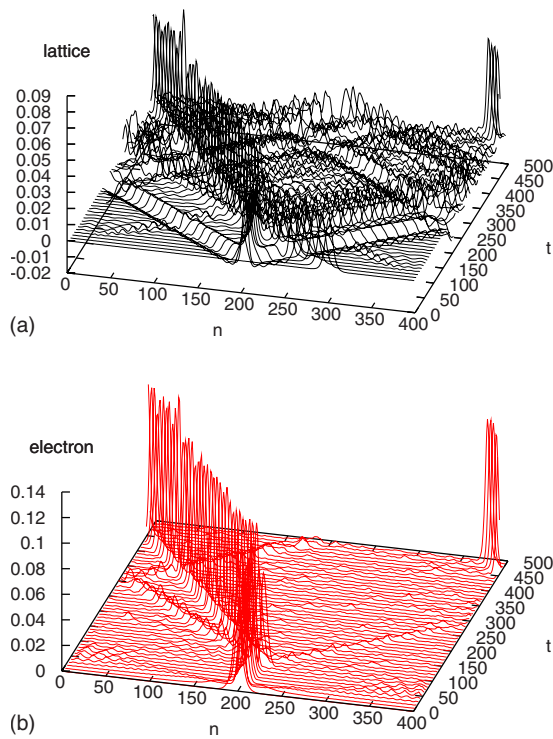


FIG. 6. (Color online) Spatiotemporal pattern of a lattice soliton (top panel) and an initially localized electron state (bottom panel). The center of the lattice soliton is initially placed at site $n=300$ while the electron is centered at site $n=200$. The parameter values are $V=0.1$ and $\alpha=1.75$.

lattice soliton have an initial distance of $\Delta n=100$. Note that this is in fact a huge distance compared with the spatial extensions of the localized electronic and solitonic lattice excitation being of the order of ten lattice sites (cf. Fig. 1). Surprisingly, the electronic occupation probability shows no sign of significant spread despite being placed in an undistorted region of the lattice. The electron preserves its localization and stays at its initial position until the traveling lattice soliton, approaching from the right, encounters the region of the lattice that is occupied by the electron. After “hitting” the electron the lattice soliton carries the electron along with it very much in the same way as described above. Crucial for the maintenance of the electronic localization is the local nonlinear interaction of the electron with the lattice vibrations due to the distance-dependence of the transfer matrix element $V_{mn-1}=V_0 \exp[-\alpha(q_n-q_{n-1})]$. To illustrate this feature Fig. 7 displays the spatiotemporal evolution of the electron and the lattice in a close neighborhood of the initial electron position. On this scale one can observe that indeed the initially strongly localized electron tends to decay. However, one recognizes that at the same time the electron induces a fairly strong local lattice compression, with $q_n - q_{n-1} < 0$, which in turn is responsible for a considerable increase of V_{mn-1} in a confined region around the electron’s position. In essence the electron gets trapped by this nonlinear lattice “impurity” [34]. Note the static character of the electron-induced lattice compression. As already noted this is akin to the polaron mechanism [35] albeit that the lattice

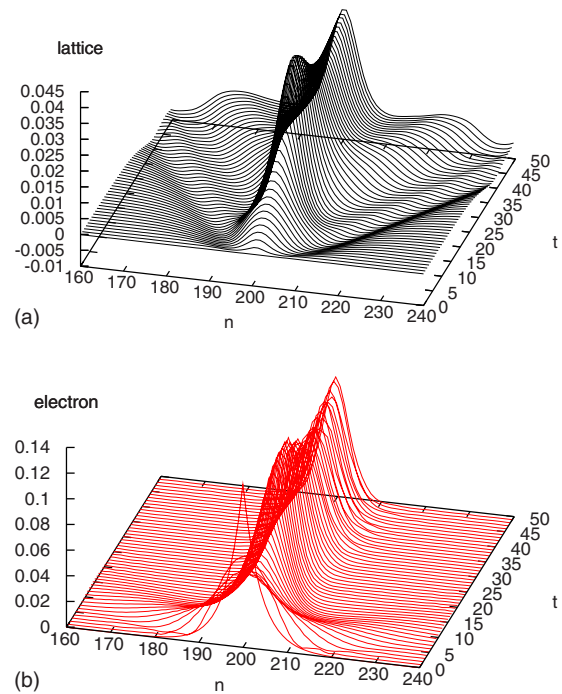


FIG. 7. (Color online) Spatiotemporal evolution of the lattice vibration (top panel) and the electronic occupation probability (bottom panel) on a segment of the lattice involving the initial position of the electron in the time interval $0 \leq t \leq 50$. Parameter values as in Fig. 6.

excitation is solitonic (nonlinear) while the genuine lattice excitation is a moving soliton. Moreover, compared with its initial state the adopted pattern of the electronic occupation probability is of even stronger degree of localization. Such a response of the lattice to the initial state of a localized electron was observed also in linear conjugated polymer chains [36].

The formation of the polaronlike state and its carriage by the traveling lattice soliton is also reflected in the time evolution of the first momentum of the electronic occupation probability and the soliton center as seen in Fig. 8. In an early phase the lattice soliton advances with comparatively high velocity towards the electron which stands still at its

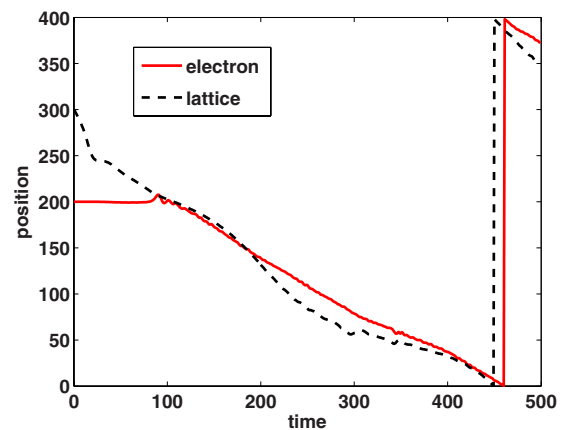


FIG. 8. (Color online) Time evolution of the electron and lattice soliton center, respectively. Parameter values as in Fig. 6.

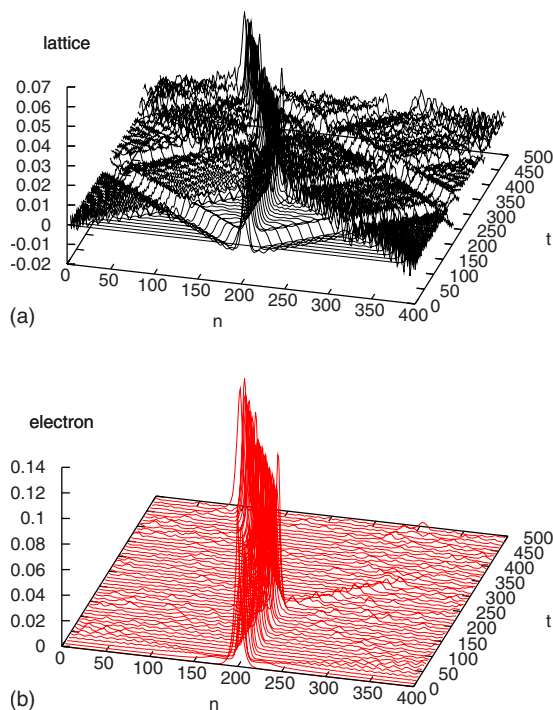


FIG. 9. (Color online) The same as in Fig. 6 except for increased initial distance between the electron and the lattice soliton of $\Delta n = 200$.

initial position. Subsequently to the formation of the standing localized lattice deformation in the proximity of the electron the velocity of the original traveling soliton lattice deformation is effectively reduced. As soon as the lattice soliton has reached the electron the two travel together with soliton velocity along the lattice.

For the case when initially the electron and the lattice soliton are 200 lattice sites apart from each other, Fig. 9 reveals that the lattice soliton travels straightforwardly towards the electron position. Again the electron manages to retain its localized shape due to the local (nonlinear) interaction with the molecules in its neighborhood. Clearly, the electron is carried away from its initial position by the pass-

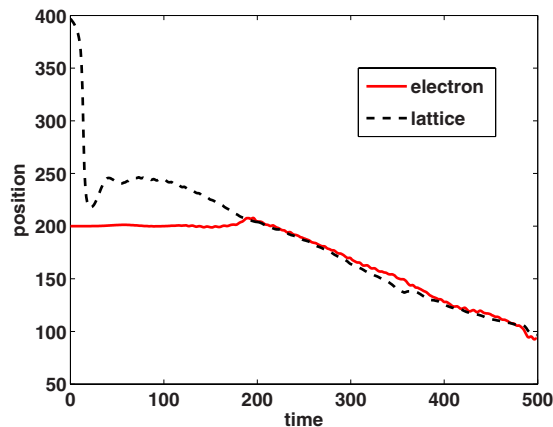


FIG. 10. (Color online) Time evolution of the electron and lattice soliton center, respectively. Parameter values as in Fig. 9.

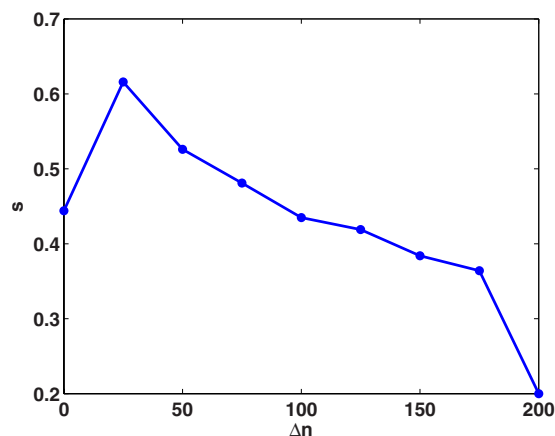


FIG. 11. (Color online) The average velocity s of the bound state in dependence of the initial distance Δn . For comparison we note that the velocity of sound in the lattice is $s=1$.

ing soliton as is also reflected in the time evolution of the center of the electron's occupation probability and the lattice soliton shown in Fig. 10.

In conclusion we have seen that even when the lattice soliton is initiated in a region far away from those sites where the electron is embedded long-range coherent electron transport is nevertheless achieved. In Fig. 11 the average velocity of the bound state, s , as a function of the initial distance Δn is depicted. Interestingly, the maximal average velocity is attained for $\Delta n=25$ and increasing the initial distance beyond this value leads to a reduction of s . For a large distance $\Delta n=200$ the bound state travels with only 20% of the velocity of sound in the bare lattice. With concern to the degree of localization and the energy exchange between the electronic and lattice degree of freedom we display in Figs. 12 and 13 the temporal behavior of the partition number $P(t)$ for different initial distances between the electron and lattice soliton and the time evolution of the partial energies, respectively. For coinciding electron and lattice soliton centers ($\Delta n=0$) $P(t)$ does not alter in long intervals apart from the early short burst where the electron and the lattice deforma-

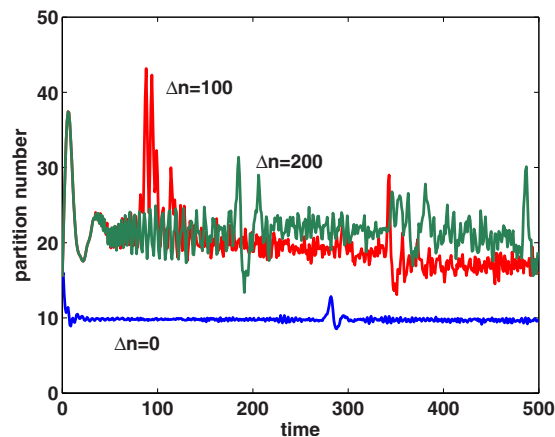


FIG. 12. (Color online) Time evolution of the electronic partition number with initial conditions and parameter values associated to Figs. 4, 6, and 9 as indicated by the value of Δn in the plot.

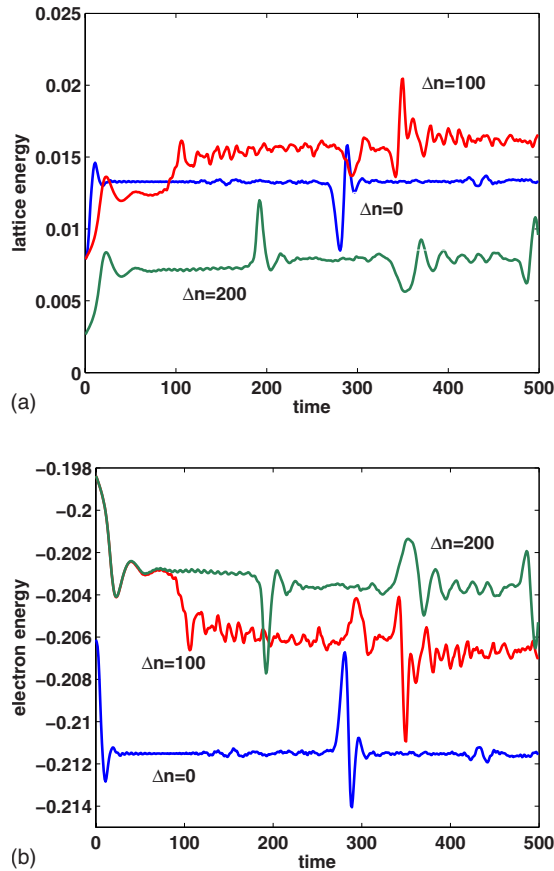


FIG. 13. (Color online) Time evolution of the partial energies for different initial distances as indicated in the plot. Top panel: H_{el} and bottom panel: $H_{lattice}$. Parameter values and initial condition as in Fig. 12.

tion adopt quickly to their mutual influence. More specifically, the electron's energy H_{el} [cf. Eq. (2)] is lowered while the lattice energy $H_{lattice}$ [cf. Eq. (3)] is raised meaning that for the motion of the localized electron-lattice compound additional deformation of the lattice is needed that has to be induced by the impact of the electron. This is a kind of polaron-soliton interaction. Apparently, the initial states are modified such that coherent motion of the localized electron-lattice deformation compound is better promoted. This goes also along with the emission of a tiny amplitude wave (the earlier mentioned phononic radiation) from the main lattice deformation soliton (cf. Fig. 4). Afterwards the corresponding separate energies stay almost constant. Around $t=280$ due to the periodic boundary conditions the emitted phonons encounter the lattice soliton leading to a brief period of energy exchange. Both the lattice soliton as well as the electron sustain this exchange period unscathed. Note that for $\Delta n=0$ the electron energy lies from the beginning below the lower edge of the linear band, $-2V_0=-0.2$, whereas for $\Delta n=100$ and 200 initially H_{el} lies within the linear band. For initial distances, $\Delta n=100$ and 200, the immediate rise of the partition number is more pronounced than in the case of $\Delta n=0$. This is due to the fact that the electron, residing at the start on an undistorted lattice segment (no polaronic effect is initially assumed), has the quantum mechanical tendency to

spread probability. However, soon the effect of the interaction with the lattice stops the spread of the electron because the lattice experiences a local (polaronic) deformation that retains to a high degree the localized shape of the wave function of the electron. Correspondingly the lattice energy increases at the expense of the electron energy (cf. Fig. 13). The latter shifts below the lower edge of the linear band. Interestingly, the amount of energy that is transferred from the electron to the lattice and the fluctuations of the partial energies are higher for the distance $\Delta n=100$ compared to $\Delta n=200$. Hence launching the lattice soliton far away from the electron's position (as in the case of $\Delta n=200$) there remains such a long time before the original soliton reaches the electron that the latter is able to create in its surrounding an appropriate lattice deformation (the polaronlike effect) so that, after the early decay, the electron restores its localization solely by itself. (Distinct to this for $\Delta n=100$ the traveling soliton lattice deformation arrives already before the formation of the polaronlike state at the electron's position could be completely finished.) Naturally, to this aim the electron has to "sacrifice" a portion of its energy to the lattice. In more detail, the time it takes for the original soliton lattice deformation to hit the standing deformation that has been built around the electron is nearly twice as long in the case of $\Delta n=200$ compared to the case $\Delta n=100$, and thus leaving in the former case more time for the formation of the localized electron-lattice compound. In particular the compression of the lattice attains for $\Delta n=200$ the form of a static kink whereas for $\Delta n=100$ the formation process proceeds not as efficient and still linear waves are being emitted from the forming localized pattern. That is the reason why for $\Delta n=100$ the interaction between the traveling soliton and the polaronlike state that is being formed around the electron's position is characterized by fairly large fluctuations of the partial energies for times $t > 100$. In contrast for $\Delta n=200$ the traveling lattice soliton encounters the pinned polaron (already having radiated dispensable linear waves) and their interference with energy exchange is virtually suppressed.

Finally, we present the spatiotemporal patterns for the case when the electron is in the beginning completely delocalized, viz. $P(0) \sim N$, and a lattice soliton is launched which moves along the lattice in Fig. 14. As far as the launching of the localized lattice deformation is concerned it can be generated, e.g., by an input pulselike excitation of mechanical, thermal, or optical origin in a lattice region [38]. Remarkably, along the path of the soliton the electron occupation probability gets increasingly concentrated in the course of time as though the traveling lattice deformation acts like a "vacuum cleaner" sweeping across the lattice to gather the electronic amplitude [reflected in the temporal behavior of the occupation number $P(t)$, cf. Fig. 15]. Eventually a fairly strongly localized electron-lattice soliton compound is formed which moves directionally along the lattice. In this sense the decay process exhibited by the independent electron on the undistorted lattice (cf. Figs. 2 and 3) has been reversed by the coupling of the electron to the traveling soliton lattice deformation. This effect of collecting the electron wave function can be (heuristically) explained as follows: In the region of the compression of the lattice it holds that $q_n - q_{n-1} < 0$. Therefore the transfer matrix element V_{nn-1}

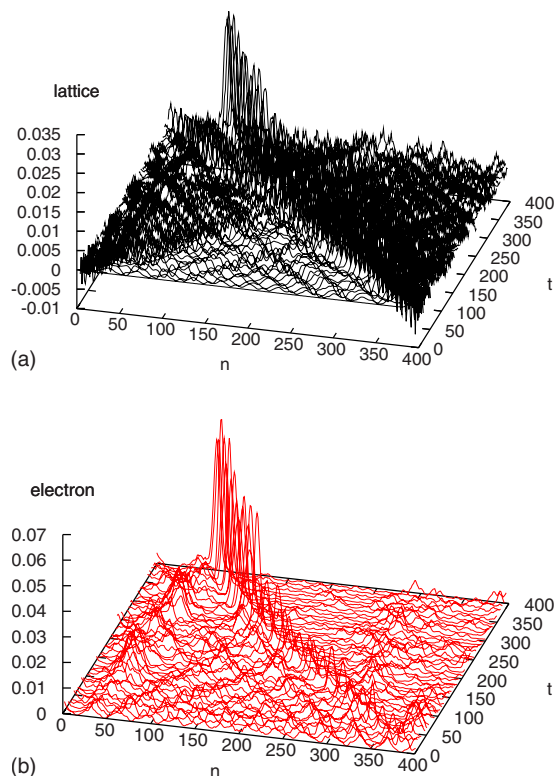


FIG. 14. (Color online) Spatiotemporal evolution of the lattice soliton (top panel) and the electronic occupation probability (bottom panel). The parameter values are $V=0.1$, $\alpha=1.75$, and $\tau=10$. At the beginning the electron is uniformly spread over the lattice and the lattice soliton is launched at site $n=400$.

$=V_0 \exp[-\alpha(q_n - q_{n-1})]$ is increased with respect to the value V_0 attained when the lattice is undistorted hence at its equilibrium configuration. In turn the local increase of the transfer matrix element is connected with local lowering of the electronic energy [see Eq. (2)]. Consequently, the electron is trapped by the traveling soliton lattice deformation (constituting a potential well) and follows the path of the latter. The classical counterpart of this picture has been thoroughly studied in Ref. [37].

IV. CONCLUDING REMARKS

In this paper we have investigated the electron transport in a one-dimensional lattice chain where the units are

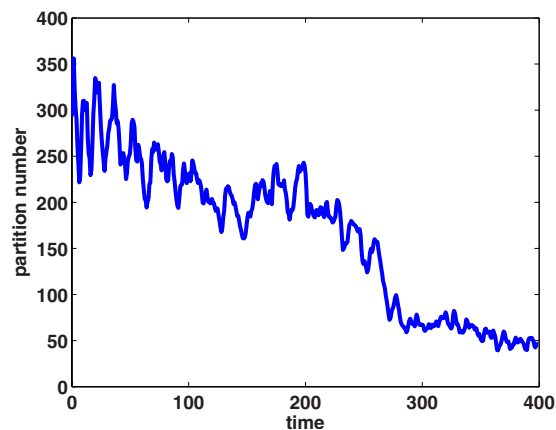


FIG. 15. (Color online) Time evolution of the electronic partition number with initial conditions and parameter values as in Fig. 14.

coupled via Morse potentials. The motion of an excess electron is described by a tight-binding Hamiltonian. The electronic transfer matrix element obeys an exponential dependence on the distance between two units. First we demonstrated that when the electron is injected into a confined region of the undistorted lattice the latter is locally such appropriately deformed in the form of a kinklike excitation that the electron is trapped forming together with the lattice deformation a (static) polaronlike state. Furthermore, we showed that the polaronlike state gets captured and subsequently dragged by a passing soliton lattice deformation. In this way coherent soliton-mediated electron transport is accomplished. Remarkably, if the electron's occupation probability is initially uniformly spread among the lattice we showed that a traveling soliton lattice deformation gathers more and more of the electronic amplitude in the course of time. Eventually the lattice soliton carries a strongly localized electron.

ACKNOWLEDGMENTS

This research has been sponsored by the European Union under Grant No. SPARK FP6-CT04-004690. One of the authors (D.H.) gratefully acknowledges support by the VW foundation via Project No. I/80425.

[1] L. D. Landau, *Phys. Z. Sowjetunion* **3**, 664 (1933).
 [2] S. I. Pekar, *Zh. Eksp. Teor. Fiz.* **16**, 336 (1946); L. D. Landau and S. I. Pekar, *ibid.* **18**, 419 (1948).
 [3] A. S. Davydov, *J. Theor. Biol.* **38**, 559 (1973); A. S. Davydov and N. I. Kislukha, *Sov. Phys. JETP* **44**, 571 (1973); A. S. Davydov, *Usp. Fiz. Nauk* **138**, 603 (1982) [*Sov. Phys. Usp.* **25**, 898 (1982)].
 [4] *Davydov's Solitons Revisited*, edited by P. L. Christiansen and A. C. Scott (Plenum Press, New York, 1991).

[5] A. C. Scott, *Phys. Rep.* **217**, 1 (1992).
 [6] A. S. Davydov, *Solitons in Molecular Systems* (Reidel, Dordrecht, 1985).
 [7] M. Toda, *Theory of Nonlinear Lattices* (Springer-Verlag, Berlin, 1991).
 [8] P. Morse, *Phys. Rev.* **34**, 57 (1929).
 [9] E. del Rio, M. G. Velarde, and W. Ebeling, *Physica A* **377**, 435 (2007).
 [10] S. Yomosa, *Phys. Rev. A* **32**, 1752 (1985).

- [11] M. G. Velarde, W. Ebeling, and A. P. Chetverikov, *Int. J. Bifurcation Chaos Appl. Sci. Eng.* **15**, 245 (2005).
- [12] A. P. Chetverikov, W. Ebeling, and M. G. Velarde, *Int. J. Bifurcation Chaos Appl. Sci. Eng.* **16**, 1613 (2006).
- [13] A. P. Chetverikov, W. Ebeling, and M. G. Velarde, *Contrib. Plasma Phys.* **45**, 275 (2005).
- [14] A. P. Chetverikov, W. Ebeling, and M. G. Velarde, *Eur. Phys. J. B* **44**, 509 (2005).
- [15] P. L. Christiansen, J. C. Eilbeck, V. Z. Enol'skii, and Yu. B. Gaididei, *Phys. Lett. A* **166**, 129 (1992).
- [16] Yu. B. Gaididei, P. L. Christiansen, and S. F. Minaleev, *Phys. Scr.* **51**, 289 (1995).
- [17] A. V. Zolotaryuk, K. H. Spatschek, and A. V. Savin, *Phys. Rev. B* **54**, 266 (1996).
- [18] R. A. Marcus, *J. Chem. Phys.* **24**, 966 (1956).
- [19] R. A. Marcus and N. Sutin, *Biochim. Biophys. Acta* **11**, 265 (1985).
- [20] D. Hennig, *Phys. Rev. E* **61**, 4550 (2000).
- [21] M. G. Velarde, W. Ebeling, D. Hennig, and C. Neißner, *Int. J. Bifurcation Chaos Appl. Sci. Eng.* **16**, 1035 (2006).
- [22] D. Hennig, C. Neißner, M. G. Velarde, and W. Ebeling, *Phys. Rev. B* **73**, 024306 (2006).
- [23] G. P. Tsironis, M. Ibanes, and J. M. Sancho, *Europhys. Lett.* **57**, 5 (2002).
- [24] B. G. Vekhter and M. A. Ratner, *J. Chem. Phys.* **101**, 9710 (1994); *Phys. Rev. B* **51**, 3469 (1995).
- [25] Ph. Choquard, *The Anharmonic Crystal* (Benjamin, New York, 1967).
- [26] N. W. Ashcroft and N. D. Mermin, *Solid State Physics* (Holt, Rinehardt and Winston, Philadelphia, 1976).
- [27] C. Kittel, *Quantum Theory of Solids* (Wiley, New York, 1987).
- [28] J. K. Freericks, M. Jarrell, and G. D. Mahan, *Phys. Rev. Lett.* **77**, 4588 (1996).
- [29] S. Flach and K. Kladko, *Phys. Rev. B* **53**, 11531 (1996).
- [30] B. Zhou and J.-Z. Xu, *J. Phys.: Condens. Matter* **10**, 7929 (1998).
- [31] Y. Zolotaryuk and J. C. Eilbeck, *J. Phys.: Condens. Matter* **10**, 4553 (1998).
- [32] G. Kalosakas, S. Aubry, and G. P. Tsironis, *Phys. Rev. B* **58**, 3094 (1998).
- [33] D. Hennig, *Phys. Rev. E* **62**, 2846 (2000).
- [34] D. Hennig, *Phys. Rev. E* **64**, 041908 (2001); *Physica A* **309**, 243 (2002).
- [35] T. Holstein, *Ann. Phys. (N.Y.)* **8**, 325 (1959).
- [36] W. P. Su and J. R. Schrieffer, *Proc. Natl. Acad. Sci. U.S.A.* **77**, 5626 (1980); W. P. Su, J. R. Schrieffer, and A. J. Heeger, *Phys. Rev. B* **22**, 2099 (1980); E. J. Mele, *ibid.* **26**, 6901 (1982); A. R. Bishop, D. K. Campbell, P. S. Lomdahl, B. Horovitz, and S. R. Phillpot, *Phys. Rev. Lett.* **52**, 671 (1984); A. R. Bishop, D. K. Campbell, P. S. Lomdahl, B. Horovitz, and S. R. Phillpot, *Synth. Met.* **9**, 223 (1984); A. J. Heeger, S. Kivelson, J. R. Schrieffer, and W. P. Su, *Rev. Mod. Phys.* **60**, 781 (1988).
- [37] V. A. Makarov, M. G. Velarde, A. Chetverikov, and W. Ebeling, *Phys. Rev. E* **73**, 066626 (2006).
- [38] A. C. Scott, *Nonlinear Science* (Oxford University Press, New York, 1999).